

Pacific Spiny Lumpsucker armor—Development, damage, and defense in the intertidal

Eleanor C. Woodruff¹  | Jonathan M. Huie²  | Adam P. Summers^{3,4}  |
 Karly E. Cohen^{3,4} 

¹Department of Biology, Carleton College, Northfield, Minnesota, USA

²Department of Biology, George Washington University, Washington, District of Columbia, USA

³Friday Harbor Laboratories, University of Washington, Friday Harbor, Washington, USA

⁴Department of Biology, University of Washington, Seattle, Washington, USA

Correspondence

Karly E. Cohen, 620 University Rd, Friday Harbor Labs, Friday Harbor, WA 98250, USA.
 Email: kecohen@uw.edu

Funding information

National Science Foundation, Grant/Award Numbers: DBI-1759637, DBI-1852096; NSF graduate research fellowship, Grant/Award Number: DGE-1746914; Eugster Endowed Student Research and Internship Fund

Abstract

Predation, combat, and the slings and arrows of an abrasive and high impact environment, represent just some of the biotic and abiotic stressors that fishes are armored against. The Pacific Spiny Lumpsucker (*Eumicrotremus orbis*) found in the subtidal of the Northern Pacific Ocean is a rotund fish covered with epidermal, cone-shaped, enamel odontodes. The Lumpsucker is a poor swimmer in the wave swept rocky intertidal, and this armor may be a lightweight solution to the problem of collisions with abiotic obstacles. We use micro-CT and scanning electron microscopy to reveal the morphology and ontogeny of the armor, and to quantify the amount of mineralization relative to the endoskeleton. The non-overlapping odontodes are organized into eight rows—six rows on the body, one row surrounding the eye, and one row underneath the chin. Odontodes start as a single, hooked cone; and they grow by the addition of cusps that accrete into a spiral. The mineral investment in armor compared to skeleton increases over ontogeny. Damage to the armor occurs both through passive abrasion and breakage from impact; and there is no evidence of replacement, or repair of damaged odontodes.

KEYWORDS

allometry, growth, odontodes, ontogeny, protection

1 | INTRODUCTION

Armor has repeatedly evolved in fishes, and serves a variety of roles, including defense, offense, display, restriction of movement, and camouflage (Buser et al., 2019; Kawai, 2019; Kolmann, Peixoto, et al., 2020; Kolmann, Urban, & Summers, 2020; Kruppert et al., 2020; Lowe et al., 2021; Porter et al., 2013; Reichert & Steffen, 2010; Sherman et al., 2017; Song et al., 2011; Yang et al., 2015). The morphology of armor, whether it is thick or thin, the presence or absence of sculpturing, and the material it is made of, can reveal function. A close examination of wear and breakage can tell some of the story of how the armor is used (Kruppert et al., 2020). Armor that has been abraded away is defending against a different assault than armor that is broken or deeply scratched. Armor represents an investment in mineral that reflects an animal's ecology and natural history; a relationship that is only revealed by a paired investigation into gross morphology and a fine scale examination of the surface plates.

Gross morphology of armor layout can hold information about its utility as a defensive structure, as well as the penalties imposed by the armor on mobility or maneuverability. For example, the lightweight armor plates, with minimal overlap, seen in sticklebacks offer less protection than the fully imbricate armor of seahorses and pipefishes (Browning, 2012; Porter et al., 2013; Song et al., 2010; Vamosi & Schluter, 2004; Webb et al., 1992). However, stickleback armor imposes a far smaller penalty on both swimming speed and turning ability. When the armor fully encases the fish there are still informative nuances—the fully fused armor of a boxfish restricts body undulation, while the rail and channel system that connects the overlapping plates of a Northern Spineless Poacher allows these fish to retain the ability to c-start (Kolmann, Peixoto, et al., 2020; Yang et al., 2015).

Armor, whether made up of dermal bone or epidermally derived odontodes such as ganoid scales, placoid scales, or denticles, bear witness to the types of damage they are subjected to. The surface will

wear with fine striations when colliding with an abrasive environment, but encounters with teeth or sharp substrates lead to wider scratches, and powerful impacts leave broken edges (Kruppert et al., 2020). Spalling, or the removal of a section of surface, is also evidence of a shearing impact. These damage modes can be quantified across or among individuals and species by a close examination of the surface, either by scanning electron microscopy (SEM) or CT scanning (Kolmann, Peixoto, et al., 2020; Kolmann, Urban, & Summers, 2020; Kruppert et al., 2020). Intact armor subjected to known damage can then be visualized for ground truthing the results in field caught specimens. Looking at damage patterns and the frequency of wear is sometimes the best way to see what the plates are made of. Broken edges may show the characteristic columnar morphology of enamel and fibrous or tubular areas of dentine. Also, armor that lacks damage suggests that the structures may be for display or may act as a substrate for epibionts that will conceal the fish from predators.

Pacific Spiny Lumpsummers (*Eumicrotremus orbis*) are small, charismatic, and densely armored fish of the North Pacific Ocean, and their armor may serve all, or most, of the previously mentioned functions (Arita, 1969; Berge & Nahrgang, 2013). They are found in the heavily fouled and rugose near-shore intertidal and subtidal environment. Because of their rotund bodies, Pacific Spiny Lumpsummers are poor

swimmers, but they have a pelvic suctorial disc that helps them stick to surfaces (Arita, 1969; Budney & Hall, 2010; Hart, 1973; Tietbohl, 2014). Male lumpsummers tend nests in evacuated barnacles covered in red coralline algae, and their whole body fluoresces in the same red as their substrate. This fluorescence, in concert with the outline breaking armor, camouflages them against the algae covered background (Cohen & Summers, in press). The spinous armor of lumpsummers may also play a defensive role as the fish face a myriad of assaults from biotic and abiotic stressors (Figure 1).

Here, we quantify the development and morphology of armor in the Pacific Spiny Lumpsummer. Our goals were fourfold: 1) describe the development of lumpsummer armor, 2) quantify the amount of mineral investment in armor relative to skeleton across ontogeny, 3) qualitatively and quantitatively assess damage to lumpsummer armor, and 4) determine the material that constitutes the armor.

2 | MATERIALS AND METHODS

We used a number of methods to investigate Pacific Spiny Lumpsummer armor. Historically the plates of the armor are referred to as tubercles (Arita, 1969). But this terminology does not reflect the

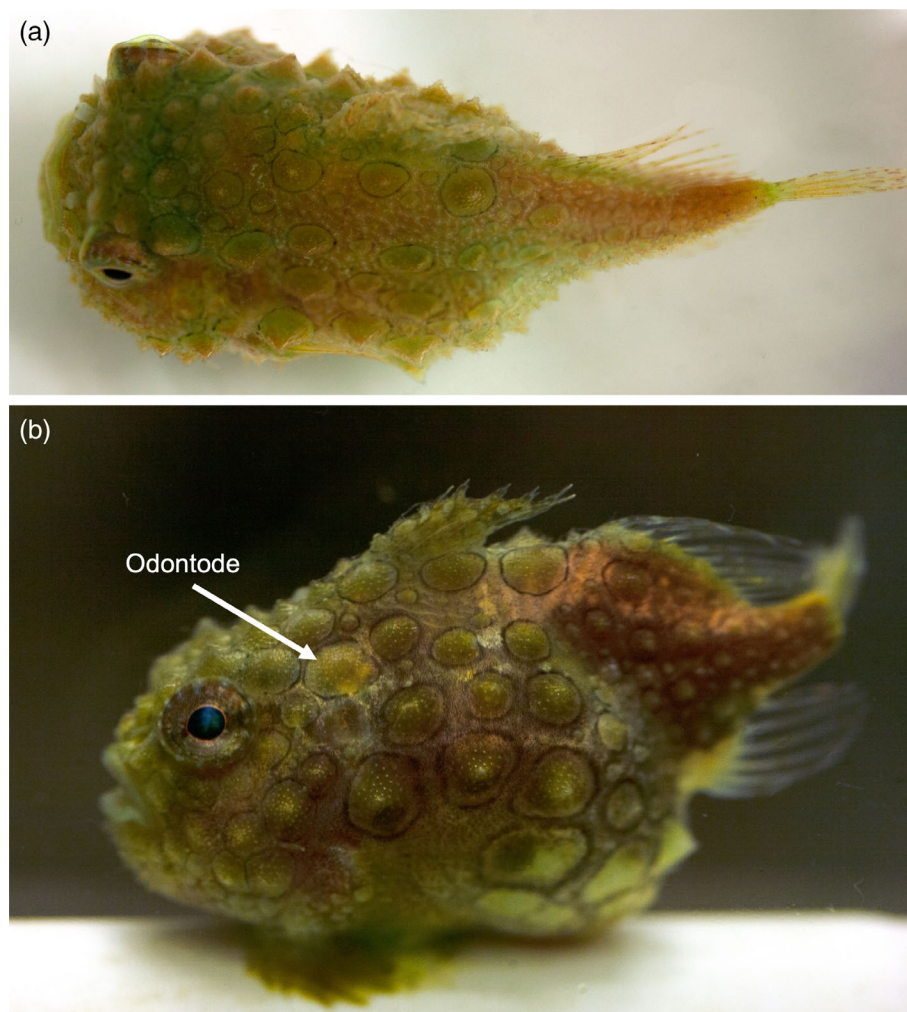


FIGURE 1 *Eumicrotremus orbis*, life images. (a) Dorsal view, (b) lateral view, displaying the cone-shaped, non-overlapping, odontodes covering the body

developmental origin, the morphology of the plates, nor their material properties. We will refer to these structures as odontodes because this term is used for any epidermal structure that contains enamel and/or dentine (Fraser et al., 2010). For example, this separates this armor from the sturgeon's dermally derived bony plates. It also makes a distinction between these structures and the keratinous breeding tubercles of cyprinid fishes, which, though sharp and cone shaped, are in no way related to Pacific Spiny Lumpsucker armor.

2.1 | Collection and CT scanning

We used micro-CT scanning to compare the morphology and mineral investment of the Pacific Spiny Lumpsucker (*E. orbis* Günther, 1861) armor across ontogeny. Specimens ($n = 39$) were obtained through the University of Washington Fish Collection, and arrived formalin-fixed and preserved in 70% EtOH. Because the specimens arrived fixed, we had no information on the animals' original color and could not sex them. This was not a problem because the armor of male and female lumpsuckers are subjected to similar abiotic factors and will likely show similar patterns of wear. All scanning was done at the Karel F. Liem Bio-Imaging Center at Friday Harbor Laboratories, Friday Harbor, WA with a Bruker Skyscan 1173. Specimens ranged from 9.2 to 97.0 mm standard length (SL) and were scanned with a voxel size between 6.1 and 35.5 μm , a voltage of 55 or 65 kV, an amperage of 123 or 133 μA , and an exposure of 1150 or 1115 ms (Table S1). We used a 1 mm Al filter for all scans to reduce attenuation artifacts. We scanned specimens together in batches of one to four, and for each batch we scanned a separate can with two standards (i.e., phantoms) with known densities (25% and 75% hydroxyapatite, respectively) at the exact same settings and resolution. Phantom scans were reconstructed in NRecon (Bruker, 2005–2011) with the same settings as their corresponding fish scans so that relative brightness of the fish could be converted into mineral density estimates. All scans used in this study were uploaded to MorphoSource.org (Table S1) and are freely available for download.

2.2 | Armor development and mineral investment

Reconstructed CT-scans were processed in the open-source image analysis software 3D Slicer (version r29738), with the SlicerMorph extension (Kikinis et al., 2014; Rolfe et al., 2021). We primarily used the thresholding and scissor tools to include all skeletal material while removing unnecessary voxels and background noise. The whole fish was separated into individual segmentation nodes consisting of only the armor and only the skeleton. We define the skeleton as a combination of both the appendicular and axial components. Volume and mean brightness of the armor and skeleton were calculated using the *Segment Statistics* tool in Slicer. We removed two individuals (84.5 and 86.5 mm SL) from our data set because either 100% or the majority of their armor was damaged or lost. To investigate the scaling relationships of armor and skeleton volume with SL, we performed

standardized major axis regressions on log-transformed data using the “lmodel2” R package (Legendre, 2018). Volume is proportional to length cubed so the predicted slope for isometric growth was 3. Scaling relationships were considered allometric if the predicted slope fell outside of the bounds of the 95% confidence intervals.

We measured bone density by comparing mean voxel brightness in each lumpsucker to the mean voxel brightness of the phantoms with known densities. We used *Segment Statistics* to find the mean voxel brightness for the 25% and 75% hydroxyapatite phantoms and derived a standard curve for each corresponding lumpsucker scan. From there, we calculated the mean concentration of hydroxyapatite in the armor and skeleton of each specimen by transforming their respective mean voxel brightnesses with the standard curves. We calculated the ratio between the concentration of hydroxyapatite in the armor and the concentration in the skeleton. We also calculated the ratio of total mineral investment in the armor versus the skeleton for each specimen. Total mineral investment was calculated by multiplying the total voxel volume of the armor and skeleton by their respective mean hydroxyapatite concentrations.

An issue that can arise when segmenting thin structures with a threshold is a partial volume effect, where intermediate gray scale voxels just miss (or just make) the threshold cutoff and skew the measure of volume in a way that is not reproducible from specimen to specimen. The odontodes certainly are thin enough to warrant concern about partial volume, but three factors mitigate against this being a significant effect. First, we scanned each fish at the best resolution for its size, so an odontode, whether on an 80 mm or 15 mm fish, had similar numbers of voxels—between 25,000 and 100,000 voxels. Second, the skeleton, like the odontodes, is without large, dense, space filling elements—instead every bone has many thin areas and sculpturing. Third, when we looked at a threshold five grayscale values darker, and five grayscale values lighter, than our selected threshold, the volume changed less than 8%. This establishes an upper bound for error in the ratio of armor to bone because the bone volume would also change with thresholding, and in the same direction.

2.3 | Assessment of damage

We divided the Pacific Spiny Lumpsucker armor into eight distinct rows to help track the growth and orientation of lumpsucker armor throughout ontogeny. These rows were initially selected by 3D-printing an oversized lumpsucker and examining the armor for patterns. We generated a hypothesis, based on our 3D-models, about the eight rows present and mapped this pattern over lumpsucker ontogeny using the micro-CT scans. In 3D Slicer, we segmented each row of armor from the left side of the fish and recorded the total number of odontodes as well as the number of damaged odontodes to track the amount and location of damage over ontogeny.

We used SEM to assess types of damage to the armor. Lumpsucker odontodes were carefully dissected away from the body and placed in a 1% trypsin solution for 24 h to let epithelial covering dissolve. Odontodes were then removed, rinsed with water, and moved through a

dehydration series in ethanol before being placed in 100% EtOH for 2 h. We removed odontodes from 100% EtOH and allowed them to dry uncovered for at least 24 h. We chose the first odontode in the fourth row, a large odontode located in the middle of the body, to compare damage and growth of an individual scale across ontogeny. These odontodes were present in our smallest individual (9.2 mm) and were easy to recognize from both the micro-CT scans and dissection. We surveyed additional odontodes that had significant damage to evaluate the extent of denticular damage. Once specimens were completely dried we sputter coated them using a Cressington 108 Sputter Coater (Ted Pella, Inc). To visualize each odontode we used a SEM (Neoscope JCM-5000). Images were taken of the whole odontode, as well as the regions of interest, including damage and cone patterns. The stage was tilted to a maximum of 45° to capture the sides of the odontode.

2.4 | Armor material

We used cross polarized microscope and SEM to determine the material basis for lump sucker odontodes. Individual scales were carefully dissected away from the body and cleaned using a 1% Trypsin solution. Cleaned odontodes were placed between the cross polarizers and

imaged using a ZEISS SteREO v20 Discovery microscope (Zeiss Oberkochen, Germany). Each piece of armor was rotated between the polarizers from when light was fully able to pass through the specimen until light was perpendicular to the direction of the mineral resulting in a black field of view. For SEM analysis, previously sampled and prepped odontodes were frozen to -80°C and broken. Cracked pieces were then remounted on SEM stubs and imaged with a Neoscope JCM-5000.

3 | RESULTS

3.1 | Investment in armor

The concentration of hydroxyapatite in Pacific Spiny Lump sucker armor versus their skeleton showed a weak positive relationship with SL ($R^2 = .2$; $p = .005$; Figure 2c). The armor: skeletal density ratio ranged from 0.72 to 1.44, though 85% of fish had nearly equal hydroxyapatite density in their armor as their skeleton (1 ± 0.2 s.e.). However, there was a relatively strong positive relationship between the armor: skeleton mineral investment ratio and SL ($R^2 = .59$, $p < .001$; Figure 2d). The total mineral (volume \times mean hydroxyapatite concentration) devoted to armor increased over ontogeny from

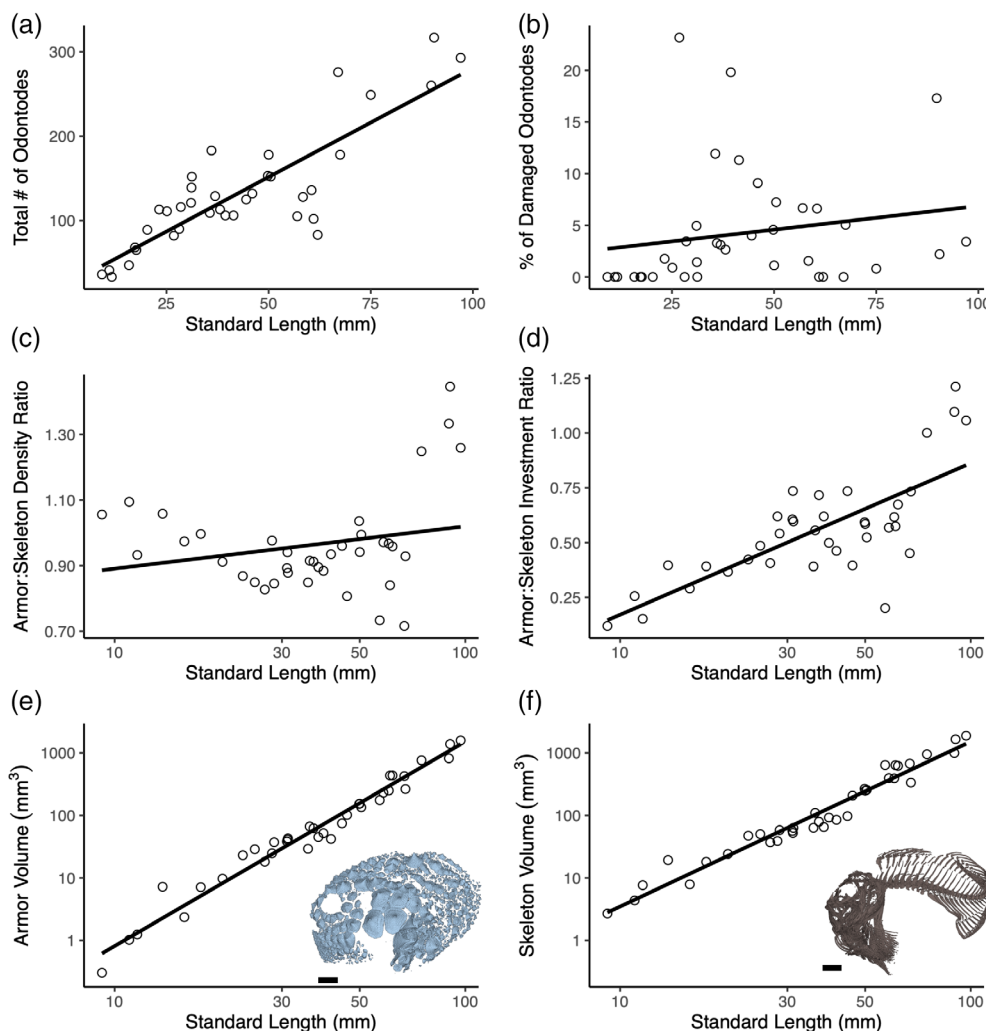


FIGURE 2 *Eumicrotremus orbis*, armor and skeletal density, investment, and volume over ontogeny. (a) Strong correlation between the total number of odontodes and standard length, and (b) weak correlation between the proportion of damaged odontodes and standard length, but the smallest individuals had no damage. (c) A slight correlation between armor density relative to skeletal density and standard length ($R^2 = .2$), (d) a strong correlation between the mineral investment in armor relative to skeletal investment and standard length ($R^2 = .59$), (e) positive allometric growth in armor volume over ontogeny ($R^2 = .97$), and (f) slight negative allometry in skeleton volume over ontogeny ($R^2 = .96$). Axes in graphs (c–f) are log transformed. Scale bar set to 1 cm

12% of the skeleton in a 9.2 mm SL fish, to 121% in a 90.5 mm SL animal (Table S2). Only large lumpstickers (89.8 mm SL–97 mm SL) invested more mineral in their armor than their skeleton. The most visibly armored fish (62 mm SL), whose armor left little unprotected, and the only fish with ventrolateral odontodes fully abutting one another, only invested half as much in its armor as in its inner skeleton. The changes in investment were primarily due to an increase in armor volume relative to the skeleton over ontogeny (Figure 2e,f). The relationship between armor volume and SL showed positive allometry over ontogeny for all individuals excluding the most heavily armored fish (slope = 3.32; 95% C.I. = 3.14–3.52, $R^2 = .97$, $p < .001$), while the skeleton volume scaled with negative allometry (slope = 2.74; 95% C.I. = 2.57–2.93, $R^2 = .96$, $p < .001$).

3.2 | Armor development

Armor develops in eight rows starting from the rostrum and extending to the caudal fin (Figures 3 and 4). Six of the rows run horizontally

along the length of the body, one runs under the orbit, and the last one is present only on the “chin” of the fish under the lower jaw. In adults, armor covered the entire body except for the most ventral part of the fish where the suction disc is located. These eight rows were not fully established in smaller lumpstickers; however, by 9.2 mm SL there was at least one scale in each of the eight partitions, and a sequence was evident in each of the rows by 11 mm SL. Armor begins developing from anterior to posterior with more odontodes on the skull and operculum than on posterior aspects of the body. As lumpstickers grow, the rows of armor are maintained and odontodes in each of those rows maintains a clear identity relative to early development (Figures 3 and 4). That is to say, odontodes do not migrate along their row or across rows as new odontodes are added, and they never overlap.

There was a positive correlation between the number of odontodes and SL ($R^2 = .71$, $p < .001$), with the largest fish (97 mm SL) having more than eight times the number of odontodes in each row than the smallest fish (9.2 mm SL, Figure 5e). There were consistently more odontodes in the first three rows of armor covering the

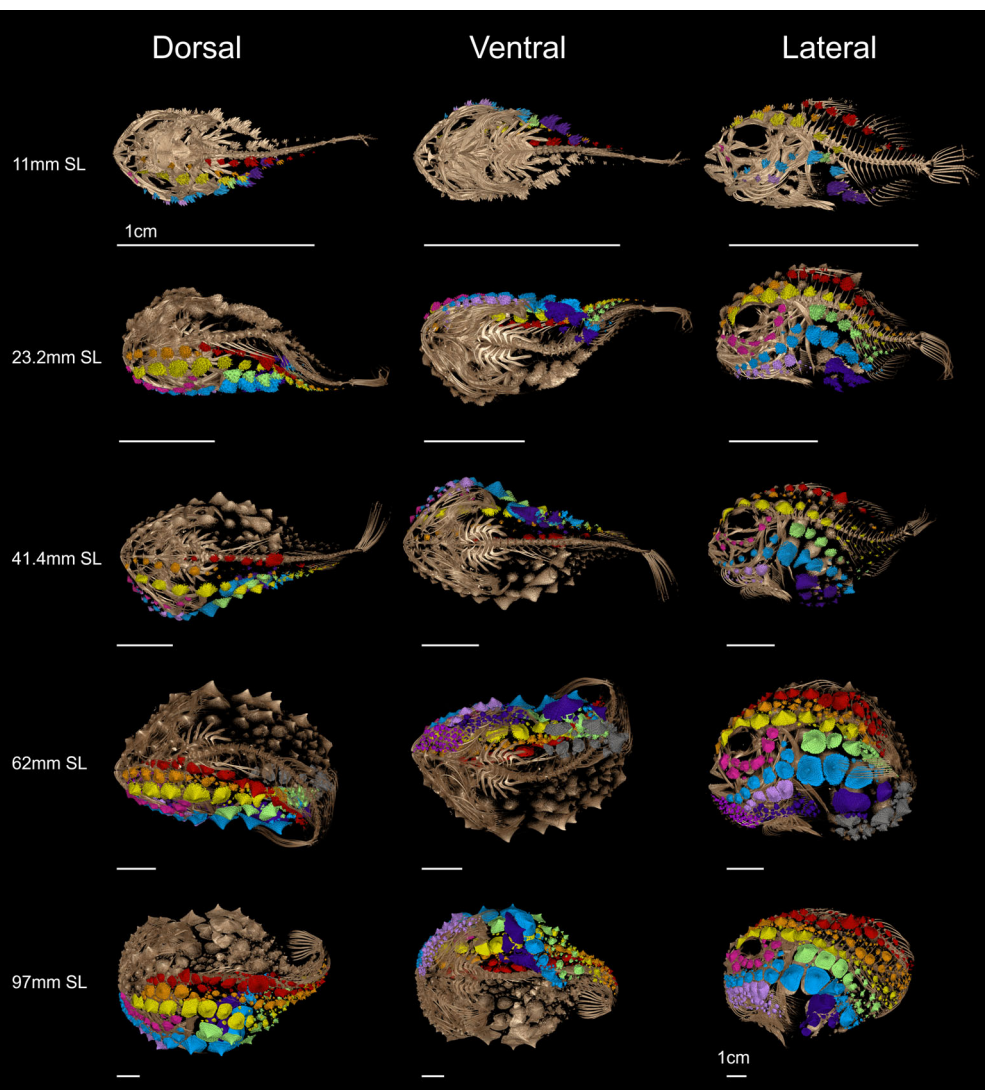


FIGURE 3 *Eumicrotremus orbis*, armor over ontogeny. Left, center, and right views showcase dorsal, ventral, and lateral aspects of lumpsticker armor. Odontodes are arranged in eight rows: Rows one through six (starting dorsally) cover the body, one runs under the eye, and one is under the chin. Scale bar is 1 cm. Different colors correspond to row numbers where row 1 = red, row 2 = orange, row 3 = yellow, row 4 = green, row 5 = blue, row 6 (eye) = pink, row 7 = indigo, row 8 (chin) = purple

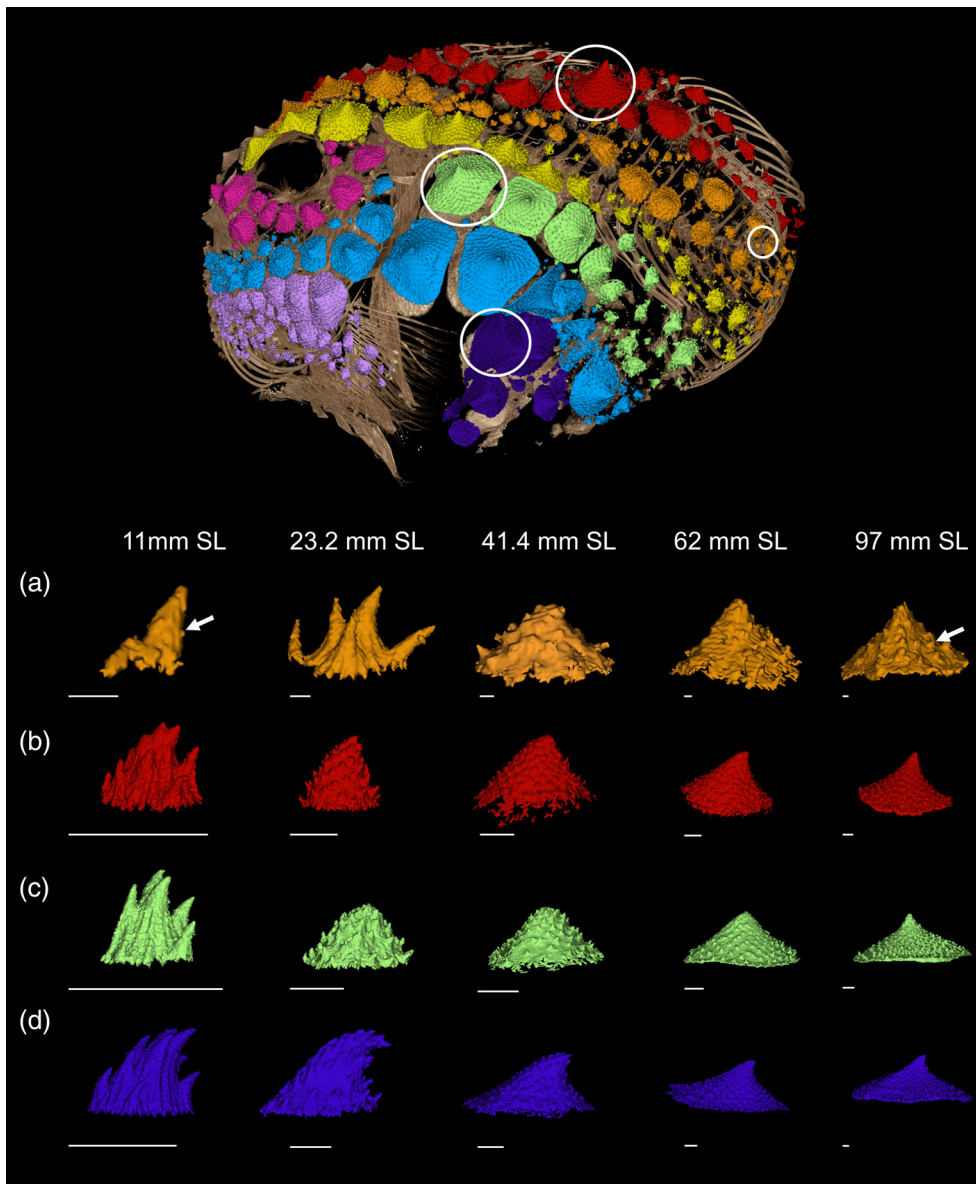


FIGURE 4 *Eumicrotremus orbis*, individual scale morphology over ontogeny. (a) Shows the morphogenesis of lumpsucker armor from a single cone to a large conical plate from row two; (b) shows the growth of the largest scale from row one; (c) shows the growth of the first scale in row four; (d) shows the growth of the first scale in row six. As the fish grows, cusps are added, eventually forming a spiral. All odontodes are shown in lateral view, scale bar is 1 mm. Arrows point to example of cones through ontogeny

neurocranium, operculum, and surrounding the eye than the rest of the body. On average, adult lumpsuckers had 19.7 odontodes in each of the first three rows, but just 17.5 in the others (Table S3). In smaller fish (11 mm SL) the first three rows had 6–8 odontodes while the rest only had 1–5 odontodes (Figure 3). In larger lumpsuckers, the first three rows were composed of numerous smaller odontodes while rows on the sides of their body had fewer odontodes that were larger. Bigger lumpsuckers have more odontodes overall on their body and in each of their rows than smaller lumpsuckers. Lumpsucker armor first develops with large odontodes, and as those structures reach their maximum size, smaller odontodes begin to fill in empty space.

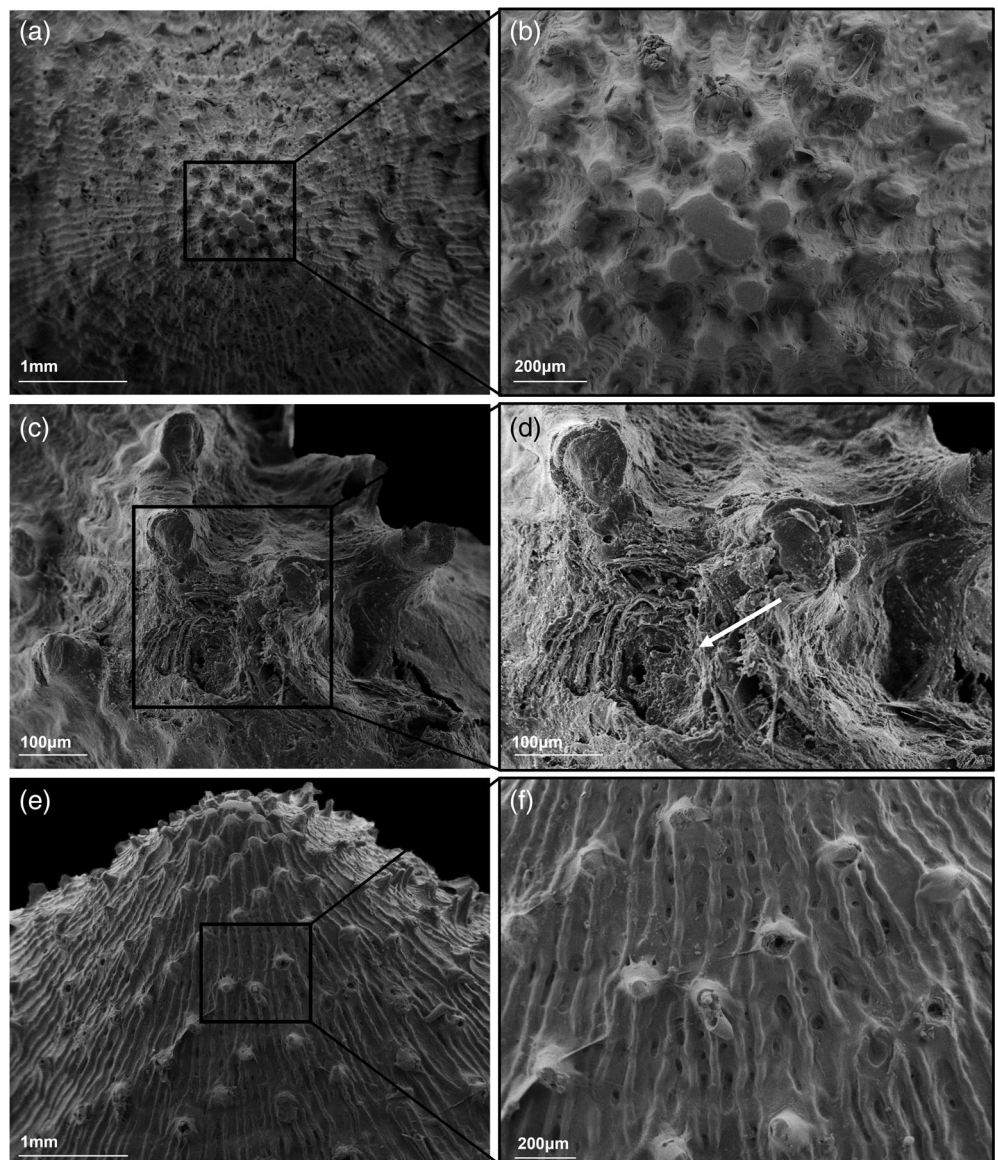
3.3 | Odontode development

The primordial Pacific Spiny Lumpsucker odontode is a single, simple cone of mineralized tissue. This cone is joined by others of varying

size and at arbitrary angles; and with each new addition, a spiral of cones becomes more apparent (Figure 4). The odontodes of smaller fish looked drastically different from the odontodes of adults. In juvenile lumpsuckers (9.2–20 mm SL), odontodes were highly topographic structures formed of aggregated cones of similar size. The aggregate made a hollow, volcano-shaped plate, but not all cones pointed straight up or in the same direction. Rather, depending on their position along the body, the cones pointed in different directions (Figure 4). Odontodes oriented in a particular direction when they are initiated stay in that direction. For instance, the largest odontode in the sixth row remained curved compared to those along the midline (Figure 4). Odontodes on the anterior end of the skeleton and the head pointed rostrally, odontodes along the midline pointed outwards, and odontodes on the posterior of the fish pointed caudally.

Odontodes begin to flatten out around 23.2 mm SL as new cones (approximately the same size as earlier ones) continue to accrete at the outer edge, and the whole structure takes on a broad-conical

FIGURE 5 *Eumicrotremus orbis*, damage of the armor. (a) Dorsal scanning electron microscopy (SEM) image of largest scale in row four, (b) inset of the odontode from image (a) showcasing abrasion damage. (c) Dorsal SEM of odontode shower complete breakage and abrasion. (d) Inset from panel (c) showcasing spalling (arrow) that resulted in severely damaged odontodes. (e) Lateral SEM image of largest scale in row four showcasing the spiraling effect of adding more cones through ontogeny, (f) inset of odontode from image (e) looking at cone breakage



shape. Odontodes maintain their hollow architecture and continue to grow. Those in the eighth row were the most curved, while those in row 4 were closest to a right circular cone (Figure 4c). Adult lump sucker odontodes (62–97 mm SL) appeared simpler than those of smaller fish because the added cones remained the same size as that first cone. Over ontogeny, the individual odontode shape is preserved, though the shape varies between rows. In a particular row, the odontodes maintain the size relationship established when they first appeared. The biggest odontode in row 8, for example, was always the largest in that row. However, rows have different growth rates: row 1 develops first, but the size of its odontodes is outstripped by those in row 4 which develop last.

3.4 | Damage and material

We observed three different types of damage to the odontodes: complete abrasion (cones are worn down to the base), partial abrasion

(tops of cones are worn down), and breakage (cones absent). These types of damage are visible in micro-CT and SEM, though partial and complete abrasion was more obvious in SEM and typically found on the top of odontodes (Figure 5a–d). We found broken cones all over the odontode, and smashed or chipped whole odontodes (Figure 5e,f). Larger fish had more damaged odontodes than smaller fish, with the five smallest fishes having no damage at all, but there was no significant correlation between damage and size ($R^2 = .005$; $p = .283$; Figure 5f). We excluded two fish (84.5 and 86.5 mm SL) where every odontode or large patches were damaged or removed, with the next most damaged fish being of average size between 25 and 40 mm SL. The two largest fish (97 mm and 90 mm SL) had fewer than 5% of their odontodes damaged (Figure 5f, Table S4). The fourth row, located in the middle of the body, had the highest proportion of damaged odontodes for any row (6%). The fourth row contained some of the largest individual odontodes and the fewest number. Odontodes under the chin had the smallest proportion of damage (1%) and were the smallest and most numerous on the body.

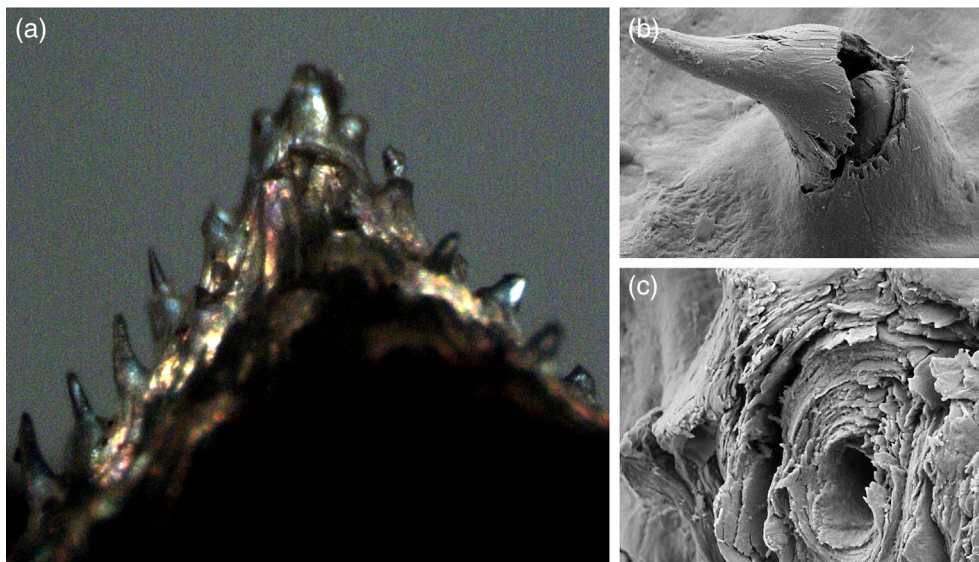


FIGURE 6 *Eumicrotremus orbis*, material of armor. (a) Cross-polarized light microscopy of adult lump sucker scale. Refraction patterns indicated that the material is not amorphous bone but rather enamel. (b and c) scanning electron microscopy (SEM) images showing the layered enamel sheets that make up lump sucker armor

SEMs of broken cones on the odontodes revealed a fibrous organization of mineralized tissue, while polarized light showed that the mineral specularly refracts light like enamel (Figure 6a). There was no evidence of repair or regrowth of broken or abraded odontodes or cones as we would expect from enamel tissue (Figure 5f).

4 | DISCUSSION

Pacific Spiny Lump sucker armor is lightweight relative to that of other fishes, like seahorses, bichirs, sea robins, boxfish, catfish, and gar (Kawai, 2019; Lowe et al., 2021; Porter et al., 2013; Reichert & Steffen, 2010; Yang et al., 2013, 2015). The largest adults invest around half of the total mineral in their body in armor, compared to more than 90% in some poachers (Agonidae) (Kruppert et al., 2020). In terms of mineral investment this is more like the highly focused defensive systems of lionfish or stingrays, where mineralized spines represent a localized defensive approach (Galloway & Porter, 2019; Shea-Vantine & Kajiura, 2021). However, the lightweight armor in lump suckers covers nearly the entire body, so it superficially appears to play as important a role as the heavy, whole-body armor of other lineages. Pacific Spiny Lump suckers live in the rocky intertidal and are poor, even comical, swimmers, powering locomotion with paired and median fin undulation (Allen & Smith, 1988; Arita, 1969; Hart, 1973). They must be at risk of collision with the structure in their habitat and they cannot evade attacks of predators. We propose that lump sucker armor represents an innovation—lightweight armor that nevertheless serves to protect against abrasion and impact.

The lack of overlap of the odontodes could indicate the armor is not proof against attack because defensive armor often has overlapping regions of high stiffness (Browning, 2012; Ehrlich, 2015; Lowe et al., 2021; Sherman et al., 2017). However, lump sucker armor bears the scars of not one, but two types of damage. Abrasion and impact leave different signatures on an armored surface. Abrasion wears away high points, leaving characteristic grooves and scratches that

can reveal the nature of the abrading surface (Amini & Miserez, 2013; Reif, 1978). Impact cleaves, or spalls, armor, leaving sharply defined edges and shatter patterns explained by the direction of the impactor (Ehrlich, 2015). Lump sucker odontodes have both types of damage suggesting both gentle and persistent abrasion wear, and that the acute stresses of impact are part of the lump sucker's life. Odontode row four, which girdles the widest part of the body, had the most damage, suggesting inadvertent contact with the substrate is an important factor. Odontodes are only abraded on the top, never along the sides, so the abrasive surface must be broad. Though lightweight, the armor is also a barrier to gape limited predators, and the cones on the odontodes would make deglutition a challenge.

As the fish grows from pea to grapefruit size, we expect collisions to be more frequent and at greater velocity. Drag and lift imposed by the complex flow of the intertidal should grow with the area of the fish, or length squared (Vogel, 2008). Forces on larger fishes will be far larger than on small ones. Inertia and collision energy are also expected to be far greater for larger individuals since both scale with mass, which is growing with the cube of length (Vogel, 2008). As a result, large Pacific Spiny Lump suckers are likely to be less able to resist currents with their poor swimming performance, leading to more collisions. The development of denticulation, and greater investment in armor, over ontogeny supports the notion that frequent and traumatic collisions become increasingly important. Smaller fish also have almost no damage, compared to some larger individuals where up to 100% of the odontodes are damaged, and are more poorly armored than larger ones, indicative of their collision-free life. Furthermore, lump suckers are unique among armored fishes in that they possess an adhesive disc that may help them reduce the chances of collision by staying put (Budney & Hall, 2010; Tietbohl, 2014).

Fish scales, whether the unadorned disks of cycloid form or the spikey plates of ctenoid form, develop first on the tail and proceed to the head (Hughes, 1981). Ctenoid scales, which have simple, conical, enamel spikes in the anterior region, start as plates of bone before sprouting spikes (Roberts, 1993; Shono et al., 2019; Williamson &

Carpenter, 1851). In contrast, the denticulated enamel cones of the Pacific Spiny Lumpsucker first develop on the head, and they manifest as a single cone. More cones are added, initially closely adherent to the first, then more widely separated by a flat area; and these form a spiral of hooked teeth on a conical surface. Like teeth, these odontodes show damage and there is no evidence they ever repair. As organisms grow and interact with their environment, we expect to see evidence of collision, predation, and defense. Armor and specialized teeth bear the most obvious scars, but enamel and dentine, the material basis for odontodes, do not repair and we see no signs of replacement of lumpsucker armor. The question then becomes how does armor stay protective as the animal grows. The answer should lie in the maintenance of a developmental pathway that ensures continuous production of odontodes but not necessarily replacements. Odontic regions in teleosts are not unheard of, for example, the denticular apparatus of ceratioid anglerfishes and the odontodes of armored catfishes (Pietsch, 2005; Schaefer & Buitrago-Suárez, 2002). Odontodes and teeth are unified by their developmental toolbox, and despite differences in regeneration or shape, all require a source of odontogenic tissue. We propose that the odontodes of lumpsuckers are of odontogenic origin and the species might be of interest in understanding the evolution and development of specialized teeth.

Overall, we find that only large lumpsuckers invest more in their armor and bigger lumpsuckers have more and larger scales. Odontodes begin as simple cones that aggregate into a flatten plate studded with smaller cones that cover the fish in eight distinct regions. The non-overlapping odontodes of Pacific Spiny Lumpsuckers may aid in camouflage against a background of rocks and barnacles while protecting this fish as it bounces through rough, subtidal waters.

ACKNOWLEDGMENTS

Special thanks to the Eugster Endowed Student Research and Internship Fund for funding to E.C.W., Stephen and Ruth Wainwright Endowment, Edwards award, Wingfield-Ramenofsky Award, and Orians Award to K.E.C., Karel F. Liem Bioimaging center, DBI-1852096, and DBI-1759637 to A.P.S., NSF Graduate Research Fellowship (DGE-1746914) to J.M.H., Katherine Maslenikov at the University of Washington Burke Museum for access to specimens.

AUTHOR CONTRIBUTIONS

Eleanor C. Woodruff: Data curation (equal); investigation (equal); visualization (equal); writing – review and editing (equal). **Jonathan M. Huie:** Conceptualization (equal); formal analysis (equal); investigation (equal); methodology (equal); validation (equal); visualization (equal); writing – review and editing (equal). **Adam P. Summers:** Funding acquisition (equal); methodology (equal); project administration (equal); resources (equal); validation (equal); writing – original draft (equal); writing – review and editing (equal). **Karly E. Cohen:** Conceptualization (lead); data curation (equal); funding acquisition (equal); investigation (equal); methodology (equal); project administration (lead); resources (equal); software (equal); supervision (equal); validation (equal); writing – original draft (equal); writing – review and editing (equal).

PEER REVIEW

The peer review history for this article is available at <https://publons.com/publon/10.1002/jmor.21435>.

DATA AVAILABILITY STATEMENT

All CT scans and data are uploaded and freely available for download at www.morphosource.org

ORCID

Eleanor C. Woodruff  <https://orcid.org/0000-0002-0996-7678>

Jonathan M. Huie  <https://orcid.org/0000-0002-7925-7372>

Adam P. Summers  <https://orcid.org/0000-0003-1930-9748>

Karly E. Cohen  <https://orcid.org/0000-0001-6556-5414>

REFERENCES

- Allen, M. J., & Smith, G. B. (1988). *Atlas and zoogeography of common fishes in the Bering Sea and northeastern Pacific* (NOAA Technical Report NMFS 66), p. 151.
- Amini, S., & Miserez, A. (2013). Wear and abrasion resistance selection maps of biological materials. *Acta Biomaterialia*, *9*, 7895–7907.
- Arita, G. S. (1969). Sexual dimorphism in the cyclopterid fish *Eumicrotremus orbis*. *Journal of the Fisheries Board of Canada*, *26*, 3262–3265.
- Berge, J., & Nahrgang, J. (2013). The Atlantic spiny lumpsucker *Eumicrotremus spinosus*: Life history traits and the seemingly unlikely interaction with the pelagic amphipod *Themisto libellula*. *Polish Polar Research*, *34*, 279–287.
- Browning, A. (2012). *Mechanics and design of flexible composite fish armor* (Thesis). Massachusetts Institute of Technology.
- Buser, T. J., Summers, A. P., & Sidlauskas, B. L. (2019). Stags of the sea? Comparisons of territoriality and cranial weapon morphology in the fish subfamily Oligocottinae (Pisces: Cottoidea). *Journal of Morphology*, *280*, S92.
- Budney, L., & Hall, B. (2010). Comparative morphology and osteology of pelvic fin-derived midline suckers in lumpfishes, snailfishes and gobies. *Journal of Applied Ichthyology*, *26*, 167–175.
- Cohen, Karly E & Summers, Adam P. Dimorphic Florescence in the Pacific Spiny Lumpsucker (In Press). *Ichthyology and Herpetology*.
- Ehrlich, H. (2015). Materials design principles of fish scales and armor. In H. Ehrlich (Ed.), *Biological materials of marine origin: Vertebrates* (pp. 237–262). Springer Netherlands.
- Fraser, G. J., Cerny, R., Soukup, V., Bronner-Fraser, M., & Streelman, J. T. (2010). The odontode explosion: The origin of tooth-like structures in vertebrates. *BioEssays*, *32*, 808–817.
- Hart, J. L. (1973). Pacific fishes of Canada. *Bulletin - Fisheries Research Board of Canada*, *180*, 740.
- Galloway K. A., Porter M. E. (2019). Mechanical properties of the venomous spines of Pterois volitans and morphology among lionfish species. *Journal of Experimental Biology*, *22*(6), jeb197905. <https://doi.org/10.1242/jeb.197905>
- Günther, A. (1861). Catalogue of the acanthopterygian fishes in the collection of the British Museum. 3. Gobiidae, Discoboli, Pediculati, Blenniidae, Labyrinthici, Mugilidae, Notacanthi. London. I-xxv + 1-586 + i-x.
- Hughes, D. R. (1981). Development and organization of the posterior field of ctenoid scales in the Platycephalidae. *Copeia*, *1981*, 596–606.
- Kawai, T. (2019). Revision of an armored searobin genus *Scaliscus* Jordan 1923 (Actinopterygii: Teleostei: Peristediidae) with a single new species. *Ichthyological Research*, *66*, 437–459.
- Kikinis, R., Pieper, S. D., & Vosburgh, K. G. (2014). 3D slicer: A platform for subject-specific image analysis, visualization, and clinical support. In *Intraoperative imaging and image-guided therapy* (pp. 277–289). Springer.

- Kolmann, M. A., Peixoto, T., Pfeiffenberger, J. A., Summers, A. P., & Donatelli, C. M. (2020). Swimming and defence: Competing needs across ontogeny in armoured fishes (Agonidae). *Journal of the Royal Society Interface*, *17*, 20200301.
- Kolmann, M. A., Urban, P., & Summers, A. P. (2020). Structure and function of the armored keel in piranhas, pacus, and their allies. *The Anatomical Record*, *303*, 30–43.
- Kruppert, S., Chu, F., Stewart, M. C., Schmitz, L., & Summers, A. P. (2020). Ontogeny and potential function of poacher armor (Actinopterygii: Agonidae). *Journal of Morphology*, *281*, 1018–1028.
- Lowe, A., Summers, A. P., Walter, R. P., Walker, S., & Misty Paig-Tran, E. W. (2021). Scale performance and composition in a small Amazonian armored catfish, *Corydoras trilineatus*. *Acta Biomaterialia*, *121*, 359–370.
- Pietsch, T. W. (2005). Dimorphism, parasitism, and sex revisited: Modes of reproduction among deep-sea ceratioid anglerfishes (Teleostei: Lophiiformes). *Ichthyological Research*, *52*, 207–236.
- Porter, M. M., Novitskaya, E., Castro-Ceseña, A. B., Meyers, M. A., & McKittrick, J. (2013). Highly deformable bones: Unusual deformation mechanisms of seahorse armor. *Acta Biomaterialia*, *9*, 6763–6770.
- Reichert, S. H., & Steffen, H. (2010). *Reverse engineering nature: Design principles for flexible protection inspired by ancient fish armor of Polypteridae* (Thesis). Massachusetts Institute of Technology.
- Reif, W. E. (1978). Protective and hydrodynamic function of the dermal skeleton of elasmobranchs. *Neues Jahrbuch für Geologie und Paläontologie Abhandlungen*, *157*, 133–141.
- Roberts, C. D. (1993). Comparative morphology of spined scales and their phylogenetic significance in the Teleostei. *Bulletin of Marine Science*, *52*, 60–113.
- Rolfe, S., Pieper, S., Porto, A., Diamond, K., Winchester, J., Shan, S., Kirveslahti, H., Boyer, D., Summers, A., & Maga, A. M. (2021). SlicerMorph: An open and extensible platform to retrieve, visualize and analyze 3D morphology. *Methods in Ecology and Evolution*, *12*, 1816–1825.
- Schaefer, S. A., & Buitrago-Suárez, U. A. (2002). Odontode morphology and skin surface features of Andean astrolepid catfishes (Siluriformes, Astrolepididae). *Journal of Morphology*, *254*, 139–148.
- Sherman, V. R., Quan, H., Yang, W., Ritchie, R. O., & Meyers, M. A. (2017). A comparative study of piscine defense: The scales of *Arapaima gigas*, *Latimeria chalumnae* and *Atractosteus spatula*. *Journal of the Mechanical Behavior of Biomedical Materials*, *73*, 1–16.
- Shea-Vantine C. S., Galloway K. A., Ingle D. N., Porter M. E., Kajiura S. M. (2021). Caudal Spine Morphology and Puncture Performance of Two Coastal Stingrays. *Integrative and Comparative Biology*, *61*, 749–758. <https://doi.org/10.1093/icb/icab077>
- Shono, T., Thiery, A. P., Cooper, R. L., Kurokawa, D., Britz, R., Okabe, M., & Fraser, G. J. (2019). Evolution and developmental diversity of skin spines in pufferfishes. *iScience*, *19*, 1248–1259.
- Song, J., Reichert, S., Kallai, I., Gazit, D., Wund, M., Boyce, M. C., & Ortiz, C. (2010). Quantitative microstructural studies of the armor of the marine threespine stickleback (*Gasterosteus aculeatus*). *Journal of Structural Biology*, *171*, 318–331.
- Song, J., Ortiz, C., & Boyce, M. C. (2011). Threat-protection mechanics of an armored fish. *Journal of the Mechanical Behavior of Biomedical Materials*, *4*, 699–712.
- Tietbohl, M. (2014). *Fishes that suck: Comparison of the adhesive discs of three fishes of the Pacific Northwest* (p. 17). Friday Harbor Laboratories.
- Vamosi, S. M., & Schluter, D. (2004). Character shifts in the defensive armor of sympatric sticklebacks. *Evolution*, *58*, 376–385.
- Vogel, S. (2008). Modes and scaling in aquatic locomotion. *Integrative and Comparative Biology*, *48*, 702–712.
- Webb, P. W., Hardy, D. H., & Mehl, V. L. (1992). The effect of armored skin on the swimming of longnose gar, *Lepisosteus osseus*. *Canadian Journal of Zoology*, *70*, 1173–1179.
- Williamson, W. C., & Carpenter, W. B. (1851). Investigations into the structure and development of the scales and bones of fishes. *Abstracts of the Papers Communicated to the Royal Society of London*, *5*, 969–971.
- Yang, W., Chen, I. H., Gludovatz, B., Zimmermann, E. A., Ritchie, R. O., & Meyers, M. A. (2013). Natural flexible dermal armor. *Advanced Materials*, *25*, 31–48.
- Yang, W., Naleway, S. E., Porter, M. M., Meyers, M. A., & McKittrick, J. (2015). The armored carapace of the boxfish. *Acta Biomaterialia*, *23*, 1–10.

SUPPORTING INFORMATION

Additional supporting information may be found in the online version of the article at the publisher's website.

How to cite this article: Woodruff, E. C., Huie, J. M., Summers, A. P., & Cohen, K. E. (2022). Pacific Spiny Lump sucker armor—Development, damage, and defense in the intertidal. *Journal of Morphology*, 1–10. <https://doi.org/10.1002/jmor.21435>